

Gapless mean-field theory of Bose–Einstein condensates

D A W Hutchinson[†], K Burnett[†], R J Dodd[†], S A Morgan[†], M Rusch[†],
E Zaremba[‡], N P Proukakis[§], Mark Edwards^{||} and C W Clark[¶]

[†] Clarendon Laboratory, Department of Physics, University of Oxford, Parks Road,
Oxford OX1 3PU, UK

[‡] Department of Physics, Queen’s University, Kingston, Ontario, Canada K7L 3N6

[§] Foundation for Research and Technology Hellas, Institute of Electronic Structure and Laser,
PO Box 1527, Heraklion 71 110, Crete, Greece

^{||} Department of Physics, Georgia Southern University, Statesboro, GA 30460-8031, USA

[¶] Electron and Optical Physics Division, National Institute of Standards and Technology,
Gaithersburg, MD 20899-8410, USA

Received 14 December 1999

Abstract. We present a topical review of the development of finite-temperature field theories of Bose–Einstein condensation in weakly interacting atomic gases. We highlight the difficulties in obtaining a consistent finite-temperature theory that has a gapless excitation spectrum in accordance with Goldstone’s theorem and which is free from both ultraviolet and infrared divergences. We present results from the two consistent theories developed so far. These are the Hartree–Fock–Bogoliubov theory within the Popov approximation and a many-body T -matrix approach which we have termed gapless-Hartree–Fock–Bogoliubov (GHFB). Comparison with the available experimental results is made and the remaining difficulties are highlighted.

(Some figures in this article are in colour only in the electronic version; see www.iop.org)

1. Introduction

The opportunity to compare quantitative microscopic theory with experimental data for many-body systems is rare. When this is possible, it often leads to the revision of long-standing theoretical notions and to the development of new, more effective theoretical methods. The experimental breakthrough in the realization of Bose–Einstein condensed gases has led to just such an opportunity [1, 2]. The predictions of finite-temperature field theory can be compared with precise experimental data.

The correct many-body theory that describes a finite-temperature, gaseous Bose–Einstein condensate (BEC) is, at present, an open question. The results of candidate theories for these systems have been successfully compared with experiment for quantities such as T -dependent condensate fractions and specific heats [3]. However, no theory has reproduced low-lying experimental collective excitation frequencies for BECs near the transition temperature [4]. In this paper we want to discuss some of the methods developed to produce quantitative predictions for a version of the mean-field theory appropriate for inhomogeneous trapped condensates. The theory we develop here is the Hartree–Fock–Bogoliubov (HFB) [5, 6] theory, consisting of a coupled set of equations; a generalized Gross–Pitaevskii equation (GPE) governing the BEC order parameter and a coupled pair of Bogoliubov–de Gennes (BdG) equations defining the quasiparticle amplitudes and energies.

We shall see that this HFB theory is able to produce excellent predictions for excitation frequencies that have been measured in the laboratory [7] for temperatures well below the transition temperature. The deviations from the predictions of the simplest versions of the theory for higher temperatures have motivated the introduction of corrections to the theory that we have recently developed. These corrections are related to improving the theory by making it conform to Goldstone's theorem [8] for systems with a spontaneously broken symmetry. The trapped gas is not a translationally invariant system so that the usual prediction of a Goldstone boson with an energy that vanishes linearly with the wavenumber of the excitation is not valid. It is possible, however, to check whether the HFB theory is consistent with the theorem in the translationally invariant limit. This brings us to an old issue in the field. The usual way to derive mean-field theory proceeds via a variational route. An alternative, but equivalent, method uses approximate factorization of higher-order correlation functions. Both routes are self-consistent yet Goldstone's theorem is not satisfied. These approaches do not yield the required zero-energy Goldstone mode. The solution to this problem is to evaluate the effective interactions, or self-energies, for the system beyond the simple variational method. This has been discussed for the translationally invariant gas. In this paper we expand upon the brief accounts of the results for the inhomogeneous system presented elsewhere and discuss the state of the art in finite-temperature field theories of this nature.

In the following section we describe in detail the development of the HFB formalism within the Popov approximation, together with results using this theory for both isotropic and anisotropic traps. These results are compared carefully with experiment and discrepancies are highlighted. In section 3 the problems encountered when trying to extend the theory beyond HFB–Popov are discussed and in section 4 the resolution to these problems is presented. This renders a new gapless HFB (GHFB) theory, results from which are presented in section 5 together with comparison to experiment. Our concluding remarks are presented in section 6. The appendix contains a comprehensive discussion of our numerical techniques.

2. HFB within the Popov approximation

2.1. Formalism

The Hamiltonian for a confined, interacting Bose gas is

$$\hat{H} = \int d\mathbf{r} \hat{\psi}^\dagger(\mathbf{r}) \left[-\frac{\hbar^2}{2m} \nabla^2 + V_{\text{ext}}(\mathbf{r}) \right] \hat{\psi}(\mathbf{r}) + \frac{1}{2} U_0 \int d\mathbf{r} \hat{\psi}^\dagger(\mathbf{r}) \hat{\psi}^\dagger(\mathbf{r}) \hat{\psi}(\mathbf{r}) \hat{\psi}(\mathbf{r}) \quad (1)$$

where $V_{\text{ext}}(\mathbf{r})$ is the external confining potential. We assume a short-range interaction with strength $U_0 = 4\pi\hbar^2 a/m$ which is determined by the *s*-wave scattering length a . We shall work in the grand canonical ensemble, in which all thermodynamic quantities are determined by the partition function

$$\mathcal{Z} = \text{Tr} e^{-\beta(\hat{H} - \mu\hat{N})} \quad (2)$$

where μ is the chemical potential. The trace operation is with respect to all many-particle states having an arbitrary number of particles N .

The field operator $\hat{\psi}(\mathbf{r})$ is now expressed in terms of an appropriate orthonormal single-particle basis

$$\hat{\psi}(\mathbf{r}) = \phi_0(\mathbf{r})\hat{a}_0 + \sum_i' \phi_i(\mathbf{r})\hat{a}_i \equiv \phi_0(\mathbf{r})\hat{a}_0 + \tilde{\psi}(\mathbf{r}) \quad (3)$$

where the destruction operators satisfy the Bose commutation relations

$$[\hat{a}_i, \hat{a}_j^\dagger] = \delta_{ij}. \quad (4)$$

The state $\phi_0(\mathbf{r})$, to be defined, has the usual significance of representing the condensate in which most of the particles reside at low temperatures. By its definition, the non-condensate field operator $\tilde{\psi}(\mathbf{r})$ has zero projection on the condensate:

$$\int d\mathbf{r} \phi_0^*(\mathbf{r}) \tilde{\psi}(\mathbf{r}) = 0. \quad (5)$$

Substituting equation (3) into equation (1) leads to an expression for the Hamiltonian which can be partitioned into terms with different numbers of the field operator $\tilde{\psi}(\mathbf{r})$. The zeroth-order term is

$$\begin{aligned} \hat{H}_0 &= \int d\mathbf{r} \phi_0^*(\mathbf{r}) \hat{T} \phi_0(\mathbf{r}) \hat{n}_0 + \frac{1}{2} U_0 \int d\mathbf{r} |\phi_0(\mathbf{r})|^4 \hat{n}_0 (\hat{n}_0 - 1) \\ &= \langle \hat{T} \rangle \hat{n}_0 + \frac{1}{2} \langle \hat{V} \rangle \hat{n}_0 (\hat{n}_0 - 1) \end{aligned} \quad (6)$$

where $\hat{T} = -\frac{\hbar^2}{2m} \nabla^2 + V_{\text{ext}}(\mathbf{r})$ is the single-particle part of the Hamiltonian and $\hat{n}_0 \equiv \hat{a}_0^\dagger \hat{a}_0$ is the number operator for the condensate. This Hamiltonian is diagonal in the non-interacting particle representation and has a common expectation value

$$E_0(N_0) = \langle \hat{T} \rangle N_0 + \frac{1}{2} \langle \hat{V} \rangle N_0 (N_0 - 1) \quad (7)$$

in each subspace having a definite number of condensate particles N_0 . The appearance of the factor $(N_0 - 1)$ accounts for the fact that there are no self-interactions between particles in the condensate. To the extent that we are dealing with states with $N_0 \gg 1$, $N_0(N_0 - 1)$ could be replaced by N_0^2 .

The term linear in $\tilde{\psi}(\mathbf{r})$ is

$$\hat{H}_1 = \int d\mathbf{r} \tilde{\psi}^\dagger(\mathbf{r}) (\hat{T} + U_0 |\phi_0(\mathbf{r})|^2 \hat{n}_0) \phi_0(\mathbf{r}) \hat{a}_0 + \int d\mathbf{r} \phi_0^*(\mathbf{r}) \hat{a}_0^\dagger (\hat{T} + U_0 |\phi_0(\mathbf{r})|^2 \hat{n}_0) \tilde{\psi}(\mathbf{r}). \quad (8)$$

We consider the following matrix element with respect to the many-particle states $|N_0; \alpha\rangle$ (an arbitrary eigenstate of \hat{n}_0):

$$\begin{aligned} \langle N'_0; \alpha' | \hat{H}_1 | N_0; \alpha \rangle &= \sqrt{N_0} \delta_{N'_0, N_0-1} \int d\mathbf{r} \langle N_0 - 1; \alpha' | \tilde{\psi}^\dagger(\mathbf{r}) | N_0 - 1; \alpha \rangle \\ &\quad \times (\hat{T} + U_0 (N_0 - 1) |\phi_0(\mathbf{r})|^2) \phi_0(\mathbf{r}) + \sqrt{N_0 + 1} \delta_{N'_0, N_0+1} \\ &\quad \times \int d\mathbf{r} \langle N_0; \alpha' | \tilde{\psi}(\mathbf{r}) | N_0; \alpha \rangle (\hat{T} + U_0 N_0 |\phi_0(\mathbf{r})|^2) \phi_0^*(\mathbf{r}). \end{aligned} \quad (9)$$

If $\phi_0(\mathbf{r})$ is chosen to be the ground state solution of

$$\left[-\frac{\hbar^2}{2m} \nabla^2 + V_{\text{ext}}(\mathbf{r}) + U_0 (N_0 - 1) |\phi_0(\mathbf{r})|^2 \right] \phi_0(\mathbf{r}) = \epsilon_0(N_0) \phi_0(\mathbf{r}) \quad (10)$$

then by virtue of equation (5), the first term on the right-hand side of equation (9) vanishes identically. To the extent that $N_0 \gg 1$, the same will be true of the second term to a good approximation, and as a result, there are no single-particle excitations from the N_0 -subspace. In other words, the truncation of the many-particle Hamiltonian to $\hat{H}_0 + \hat{H}_1$ with the choice of equation (10), leads to a reduced Hamiltonian given by equation (6) which commutes with \hat{n}_0 and therefore admits eigenstates having a definite number of particles N_0 . The remaining terms in the many-body Hamiltonian of course carry one out of a particular N_0 -subspace, but following the usual practice in Bose condensed systems, these terms are approximated in such a way as to conserve the number of particles in the condensate. As stated previously, the appearance of the factor $(N_0 - 1)$ in equation (10) rather than N_0 corrects for particle

self-interactions. However, if $N_0 \gg 1$ the difference is immaterial, and the replacement of $(N_0 - 1)$ by N_0 then yields the usual form of the Gross–Pitaevskii equation.

To explore the implications of this further, we consider the simplest approximation of replacing the full Hamiltonian, equation (1), by equation (6). The partition function in this reduced space is

$$\begin{aligned} \mathcal{Z}_0 &= \text{Tr} e^{-\beta(\hat{H}_0 - \mu_0 \hat{n}_0)} \\ &= \sum_{N_0=0}^{\infty} \exp\{-\beta[E_0(N_0) - \mu_0 N_0]\} \end{aligned} \quad (11)$$

where μ_0 is the condensate only approximation to μ . The maximum contribution will come from the region where the exponent is minimized, namely

$$\mu_0 = \frac{dE_0(\bar{N}_0)}{d\bar{N}_0}. \quad (12)$$

This is the defining equation for the condensate only chemical potential in terms of the expected number of particles in the condensate, \bar{N}_0 . Two alternatives in the evaluation of equation (12) are available: (a) $\phi_0(\mathbf{r})$ is allowed to vary with N_0 in the evaluation of the matrix elements in equation (7) and (b) $\phi_0(\mathbf{r})$ is determined for \bar{N}_0 condensate particles and is held fixed. $E_0(N_0)$ then has only the explicit N_0 dependence shown in equation (7). This latter case corresponds to choosing a fixed single-particle basis which is independent of the number of particles in the system.

In case (a), equation (10) can be used to express the expectation value of \hat{T} in terms of the eigenvalue and we have

$$E_0(N_0) = \epsilon_0(N_0)N_0 - \frac{1}{2}N_0(N_0 - 1)\langle\hat{V}\rangle. \quad (13)$$

Using

$$\frac{d\epsilon_0(N_0)}{dN_0} = \langle\hat{V}\rangle + \frac{1}{2}(N_0 - 1)\frac{d\langle\hat{V}\rangle}{dN_0} \quad (14)$$

which follows from equation (10), we obtain

$$\mu_0 = \epsilon_0(\bar{N}_0) + \frac{1}{2}\overline{\langle\hat{V}\rangle}. \quad (15)$$

The bar is a reminder that the matrix element is evaluated with a condensate wavefunction corresponding to \bar{N}_0 particles. The first term dominates since it contains the contribution $(\bar{N}_0 - 1)\langle\hat{V}\rangle$, and μ_0 is thus the condensate eigenvalue to $O(\bar{N}_0)$. The term $\langle\hat{V}\rangle/2$ can be traced to the self-interaction correction. Omitting this correction, the same analysis would lead to $\mu_0 = \epsilon_0(\bar{N}_0)$ without the extra term. For the second case, we have

$$\begin{aligned} \frac{dE_0(N_0)}{dN_0} &= \overline{\langle\hat{T}\rangle} + (N_0 - \frac{1}{2})\overline{\langle\hat{V}\rangle} \\ &= \epsilon_0(\bar{N}_0) + \frac{1}{2}\overline{\langle\hat{V}\rangle} + (N_0 - \bar{N}_0)\overline{\langle\hat{V}\rangle}. \end{aligned} \quad (16)$$

Setting this equal to the value of μ_0 given by equation (15), we find that the expected number of condensate particles is $N_0 = \bar{N}_0$, the same result as found by allowing $\phi_0(\mathbf{r})$ to vary with N_0 .

To go beyond the Gross–Pitaevskii description requires a treatment of the higher-order terms (\hat{H}_2 , \hat{H}_3 and \hat{H}_4) so far neglected. For \hat{H}_2 we have

$$\begin{aligned}\hat{H}_2 &= \int d\mathbf{r} \tilde{\psi}^\dagger(\mathbf{r})[\hat{T} + 2U_0|\phi_0(\mathbf{r})|^2\hat{n}_0]\tilde{\psi}(\mathbf{r}) \\ &\quad + \frac{1}{2}U_0 \int d\mathbf{r} [\hat{a}_0^2\phi_0(\mathbf{r})^2\tilde{\psi}^\dagger(\mathbf{r})\tilde{\psi}^\dagger(\mathbf{r}) + \hat{a}_0^{\dagger 2}\phi_0^*(\mathbf{r})^2\tilde{\psi}(\mathbf{r})\tilde{\psi}(\mathbf{r})] \\ &\simeq \int d\mathbf{r} \tilde{\psi}^\dagger(\mathbf{r})[\hat{T} + 2U_0n_c(\mathbf{r})]\tilde{\psi}(\mathbf{r}) \\ &\quad + \frac{1}{2}U_0 \int d\mathbf{r} [\Phi(\mathbf{r})^2\tilde{\psi}^\dagger(\mathbf{r})\tilde{\psi}^\dagger(\mathbf{r}) + \Phi^*(\mathbf{r})^2\tilde{\psi}(\mathbf{r})\tilde{\psi}(\mathbf{r})].\end{aligned}\quad (17)$$

In keeping with the idea of a fixed condensate number N_0 , we have replaced the \hat{a}_0 and \hat{a}_0^\dagger operators by the c -number $\sqrt{N_0}$, and have defined the condensate wavefunction

$$\Phi(\mathbf{r}) = \sqrt{N_0}\phi_0(\mathbf{r}) \quad (18)$$

and condensate density

$$n_c(\mathbf{r}) = |\Phi(\mathbf{r})|^2. \quad (19)$$

For \hat{H}_3 we have

$$\hat{H}_3 \simeq 2U_0 \int d\mathbf{r} \tilde{\psi}^\dagger(\mathbf{r})\tilde{n}(\mathbf{r})\phi_0(\mathbf{r})\hat{a}_0 + 2U_0 \int d\mathbf{r} \phi_0^*(\mathbf{r})\hat{a}_0^\dagger\tilde{n}(\mathbf{r})\tilde{\psi}(\mathbf{r}). \quad (20)$$

In arriving at this result, we have used a Hartree–Fock factorization of the product of three $\tilde{\psi}$ operators, retaining only the average

$$\tilde{n}(\mathbf{r}) \equiv \langle \tilde{\psi}^\dagger(\mathbf{r})\tilde{\psi}(\mathbf{r}) \rangle \quad (21)$$

and neglecting the anomalous average $\langle \tilde{\psi}(\mathbf{r})\tilde{\psi}(\mathbf{r}) \rangle$. This simplification is the Popov approximation. A comparison of equation (20) with equation (8) shows that the two equations have the same form and their sum can be eliminated by a generalization of equation (10),

$$\left[-\frac{\hbar^2}{2m}\nabla^2 + V_{\text{ext}}(\mathbf{r}) + U_0[n_c(\mathbf{r}) + 2\tilde{n}(\mathbf{r})] \right] \Phi(\mathbf{r}) = \epsilon_0(N_0)\Phi(\mathbf{r}) \quad (22)$$

in which the condensate wavefunction is coupled to the non-condensate density $\tilde{n}(\mathbf{r})$. The displayed dependence of ϵ_0 on N_0 signifies the normalization of the condensate wavefunction, however, ϵ_0 also depends implicitly on other parameters through the appearance of $\tilde{n}(\mathbf{r})$ in equation (22). Similarly, we have

$$\hat{H}_4 \simeq 2U_0 \int d\mathbf{r} \tilde{n}(\mathbf{r})\tilde{\psi}^\dagger(\mathbf{r})\tilde{\psi}(\mathbf{r}) \quad (23)$$

which can be combined with \hat{H}_2 to give the total grand canonical Hartree–Fock Hamiltonian

$$\hat{K}_{\text{HF}} = \int d\mathbf{r} \tilde{\psi}^\dagger(\mathbf{r})\hat{\mathcal{L}}\tilde{\psi}(\mathbf{r}) + \frac{1}{2}U_0 \int d\mathbf{r} [\Phi(\mathbf{r})^2\tilde{\psi}^\dagger(\mathbf{r})\tilde{\psi}^\dagger(\mathbf{r}) + \Phi^*(\mathbf{r})^2\tilde{\psi}(\mathbf{r})\tilde{\psi}(\mathbf{r})] \quad (24)$$

with

$$\hat{\mathcal{L}} = \hat{T} + 2U_0n(\mathbf{r}) - \mu \quad (25)$$

and

$$n(\mathbf{r}) = n_c(\mathbf{r}) + \tilde{n}(\mathbf{r}). \quad (26)$$

The appearance of μ in equation (25) is due to the subtraction of $\mu\hat{N}$ from the Hamiltonian as required in the calculation of the partition function.

The operator \hat{K}_{HF} can be diagonalized with the usual Bogoliubov transformation

$$\tilde{\psi}(\mathbf{r}) = \sum_i [u_i(\mathbf{r})\hat{\alpha}_i - v_i^*(\mathbf{r})\hat{\alpha}_i^\dagger] \quad (27)$$

where the operators $\hat{\alpha}_i$ and $\hat{\alpha}_i^\dagger$ satisfy Bose commutation relations. Equation (24) reduces to

$$\hat{K}_{\text{HF}} = \sum_i E_i \hat{\alpha}_i^\dagger \hat{\alpha}_i - \sum_i E_i \int d\mathbf{r} |v_i(\mathbf{r})|^2 \quad (28)$$

if the functions $u_i(\mathbf{r})$ and $v_i(\mathbf{r})$ satisfy the coupled Bogoliubov–de Gennes equations

$$\begin{aligned} \hat{L}u_i(\mathbf{r}) - U_0 n_c(\mathbf{r})v_i(\mathbf{r}) &= E_i u_i(\mathbf{r}) \\ \hat{L}v_i(\mathbf{r}) - U_0 n_c(\mathbf{r})u_i(\mathbf{r}) &= -E_i v_i(\mathbf{r}). \end{aligned} \quad (29)$$

These equations define the quasiparticle excitations E_i . Together with equation (22) these constitute the HFB theory within the Popov approximation.

Quasiparticle expectation values are defined by

$$\langle \hat{O} \rangle \equiv \frac{1}{\mathcal{Z}'} \text{Tr}' \hat{O} e^{-\beta \hat{K}_{\text{HF}}} \quad (30)$$

where the quasiparticle partition function, \mathcal{Z}' , is determined by taking a trace over quasiparticle states for fixed N_0 :

$$\begin{aligned} \mathcal{Z}' &= \text{Tr}' \exp(-\beta \hat{K}_{\text{HF}}) \\ &= \exp \left\{ - \sum_i \left[\ln(1 - e^{-\beta E_i}) - \beta \int d\mathbf{r} E_i |v_i(\mathbf{r})|^2 \right] \right\} \\ &\equiv \exp\{-\beta \tilde{E}(N_0, \mu)\}. \end{aligned} \quad (31)$$

Here, $\tilde{E}(N_0, \mu)$ can be thought of as the quasiparticle contribution to the total energy. It is first a function of N_0 as a result of the choice of the normalization of the condensate wavefunction in equation (22) and second, a function of μ through its explicit appearance in the definition of \hat{L} . As an example of equation (30), the expectation value of the quasiparticle number operator is

$$\langle \hat{\alpha}_i^\dagger \hat{\alpha}_i \rangle = \frac{1}{e^{\beta E_i} - 1} \equiv N_{\text{Bose}}(E_i) \quad (32)$$

with which we obtain the non-condensate density

$$\tilde{n}(\mathbf{r}) = \sum_i \{ [|u_i(\mathbf{r})|^2 + |v_i(\mathbf{r})|^2] N_{\text{Bose}}(E_i) + |v_i(\mathbf{r})|^2 \}. \quad (33)$$

To finally determine various physical quantities, we must evaluate the total partition function

$$\mathcal{Z} = \sum_{N_0=0}^{\infty} \exp\{-\beta[E_0(N_0, \mu) + \tilde{E}(N_0, \mu) - \mu N_0]\}. \quad (34)$$

The condensate energy $E_0(N_0, \mu)$ is still defined by equation (7), but with the expectation values evaluated using the solution of equation (22). It now depends on μ through its dependence on the condensate wavefunction. Following the discussion leading to equation (12), the chemical potential is determined by

$$\mu = \left(\frac{\partial E_0(\bar{N}_0, \mu)}{\partial \bar{N}_0} \right)_\mu + \left(\frac{\partial \tilde{E}(\bar{N}_0, \mu)}{\partial \bar{N}_0} \right)_\mu \quad (35)$$

which implicitly defines the expected number of particles in the condensate, $\bar{N}_0(\mu)$, as a function of μ . For this value of \bar{N}_0 , the number of particles out of the condensate is given by

$$\tilde{N}(\bar{N}_0, \mu) = \sum_i \frac{1}{e^{\beta E_i(\bar{N}_0, \mu)} - 1} \quad (36)$$

and the total number of particles in the system is

$$N = \bar{N}_0(\mu) + \tilde{N}(\bar{N}_0(\mu), \mu). \quad (37)$$

The parameter μ must be adjusted to yield the desired number of particles, N .

The above procedure is quite involved because of the intricate interdependence of all of the quantities. The procedure simplifies when the number of particles out of the condensate satisfies $\tilde{N} \ll \bar{N}_0$. In this case, $\tilde{n}(\mathbf{r})$ is a small correction to equation (22) and the first term in equation (35) can be approximated by the condensate eigenvalue ϵ_0 . Likewise, the quasiparticle energy $\tilde{E}(N_0, \mu)$ will be small relative to $E_0(N_0, \mu)$ and as a result, the second term in equation (35) can be neglected. The approximation $\mu \simeq \epsilon_0(N_0)$ makes the quasiparticle energies an implicit function of N_0 alone, and once N_0 is fixed, so too is \tilde{N} in equation (36). This prescription, however, must fail at sufficiently large temperatures when the non-condensate number is comparable to N_0 . For example, \tilde{N} as given by equation (36) will not have an upper bound as a function of T , regardless of the value of N_0 , and may, in fact, exceed the total number of particles N . Thus the simplified treatment of setting μ equal to ϵ_0 is restricted to small degrees of excitation from the condensate, and the more elaborate procedure summarized above must be used at elevated temperatures approaching the critical temperature T_c .

We now proceed with the solution of the BdG equations. We write the operator $\hat{\mathcal{L}}$ as

$$\hat{\mathcal{L}} \equiv \hat{h}_0 + U_0 n_c(\mathbf{r}) - \mu \quad (38)$$

where \hat{h}_0 is the Hamiltonian defining the condensate wavefunction in equation (22). As we shall see, the eigenfunctions of this Hamiltonian provide a particularly convenient basis of states.

Rather than dealing with the functions u_i and v_i , it is convenient to define the functions [3]

$$\psi_i^{(\pm)}(\mathbf{r}) \equiv u_i(\mathbf{r}) \pm v_i(\mathbf{r}). \quad (39)$$

These functions are solutions of the uncoupled equations

$$(\hat{h}_0 - \mu)^2 \psi_i^{(+)}(\mathbf{r}) + 2U_0 n_c(\mathbf{r})(\hat{h}_0 - \mu) \psi_i^{(+)}(\mathbf{r}) = E_i^2 \psi_i^{(+)}(\mathbf{r}) \quad (40)$$

$$(\hat{h}_0 - \mu)^2 \psi_i^{(-)}(\mathbf{r}) + 2U_0(\hat{h}_0 - \mu) n_c(\mathbf{r}) \psi_i^{(-)}(\mathbf{r}) = E_i^2 \psi_i^{(-)}(\mathbf{r}) \quad (41)$$

and are related to each other by $(\hat{h}_0 - \mu) \psi_i^{(+)} = E_i \psi_i^{(-)}$. Equations (40) and (41) defines the collective excitations of the condensate. The numerical methods used to solve the HFB–Popov equations are discussed in the appendix.

2.2. Results for an isotropic trap

To illustrate this method it is convenient to consider a spherically symmetric harmonic trap. In this case, the Hamiltonian \hat{h}_0 is separable and the basis functions in equation (A3) take the form

$$\phi_{nlm}(\mathbf{r}) = R_{nl}(r)Y_{lm}(\hat{\mathbf{r}}) \quad (42)$$

where $Y_{lm}(\hat{\mathbf{r}})$ is a spherical harmonic and $R_{nl}(r)$ is the solution of the radial equation. The corresponding eigenvalues ε_{nl} are $(2l + 1)$ -fold degenerate. The excited state modes can likewise be classified by the angular momentum quantum numbers l and m and a radial index ν . This implies that the expansions in equations (A4) and (A8) are restricted to terms with angular components $Y_{lm}(\hat{\mathbf{r}})$ and a summation over the radial index n . However, due to the spherical symmetry, the expansion coefficients $c_\alpha^{(i)} \equiv c_n^{(vl)}$ depend on l but are independent of m . Equations (A15) and (A16) then take the form

$$\tilde{n}_1(r) = \frac{1}{8\pi} \sum_{\nu l} (2l + 1) \left\{ \left| \sum_n c_n^{(vl)} R_{nl}(r) \right|^2 + \left| \sum_n \frac{\varepsilon_{nl}}{E_{\nu l}} c_n^{(vl)} R_{nl}(r) \right|^2 \right\} N_{\text{Bose}}(E_{\nu l}) \quad (43)$$

and

$$\tilde{n}_2(r) = \frac{1}{16\pi} \sum_{\nu l} (2l + 1) \left| \sum_n \left(1 - \frac{\varepsilon_{nl}}{E_{\nu l}} \right) c_n^{(vl)} R_{nl}(r) \right|^2. \quad (44)$$

We now consider the specific isotropic harmonic potential $V_{\text{ext}}(\mathbf{r}) = \frac{1}{2}m\omega_0^2 r^2$. In addition, we use the following parameters [1, 7]: $m(^{87}\text{Rb}) = 1.44 \times 10^{-25}$ kg, $\nu_0 = \omega_0/2\pi = 200$ Hz and an s-wave scattering length of $a \simeq 110 a_0 = 5.82 \times 10^{-9}$ m. Throughout we express lengths and energies in terms of the characteristic oscillator length $d = (\hbar/m\omega_0)^{1/2} = 7.62 \times 10^{-7}$ m and the characteristic trap energy $\hbar\omega_0 = 1.32 \times 10^{-31}$ J, respectively. A convenient dimensionless parameter [9–11] describing the effective strength of the interactions is $\gamma \equiv Na/d$, which is proportional to the ratio of the average interaction energy $U_0\bar{n}$ (where $\bar{n} = N/d^3$) to the characteristic energy level spacing $\hbar\omega_0$. In the absence of $\tilde{n}(\mathbf{r})$ in equations (22) and (29), the various properties of the condensate scale [9, 10] with this single parameter γ .

For a spherical trap, the eigenfunctions of \hat{h}_0 and the quasiparticle excitations can be classified according to the angular momentum l . The number of excitations generated for a given l is determined by the dimension of the eigenfunction expansion and is chosen sufficiently large to ensure convergence of the non-condensate density as determined by the sum over all modes in equation (33).

The first point of interest is the $T = 0$ quantum depletion given by $\tilde{n}_2(r)$. The integrated value of this, \tilde{N}_2 , does not exceed 0.5% of the total number of atoms for the range of N considered and the parameters given above. Having most of the atoms in the condensate is in sharp contrast with the situation in superfluid ^4He where 90% of the atoms are outside the condensate even at $T = 0$. The monotonic increase of \tilde{N} with N is due to the dependence of the coupling between the u and v functions in the HFB–Popov equations on the effective interaction strength γ . The latter increases with N and therefore leads to an increasing number of excitations out of the condensate. Since \tilde{N} is a small fraction of the total at $T = 0$, it is to a very good approximation a function of the single parameter γ .

With increasing temperature, the non-condensate density increases by virtue of the Bose distribution term in equation (33). We note that $\tilde{n}_2(\mathbf{r})$ depends weakly on temperature and is rapidly dominated by $\tilde{n}_1(\mathbf{r})$ at elevated temperatures. In figure 1(a), we show our self-consistent results for $\tilde{n}(\mathbf{r})$ for $N = 2000$ atoms for a range of temperatures below the transition

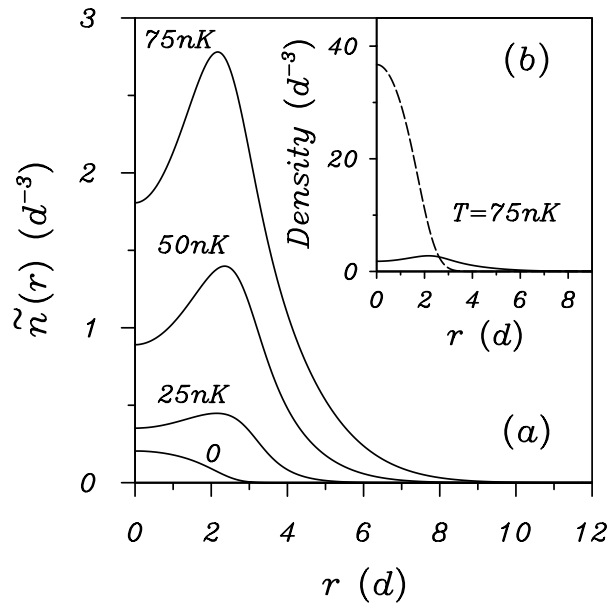


Figure 1. (a) Non-condensate density for 2000 rubidium atoms at various temperatures. (b) The non-condensate (full curve) and condensate (broken curve) densities at $T = 75$ nK [3].

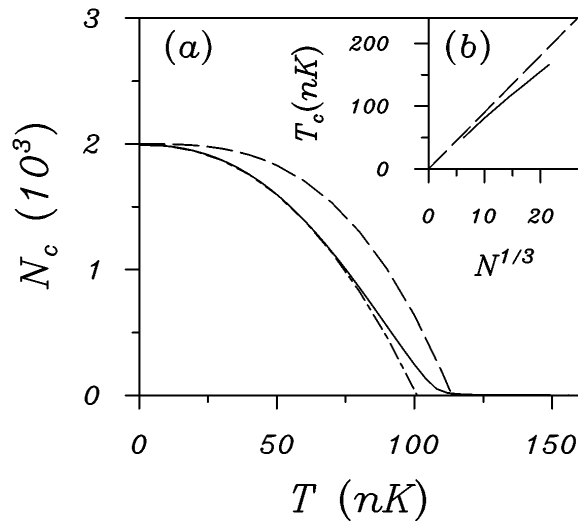


Figure 2. (a) The number of atoms within the condensate for $N = 2000$, as a function of temperature. The full curve is the result calculated using the HFB–Popov equations and the broken curve is the ideal Bose gas result, $N_c^0/N = 1 - (T/T_c^0)^3$, with $T_c^0 = (\hbar\omega_0/k_B)(N/\zeta(3))^{1/3}$. The chain curve is the fit discussed in the text. (b) The critical temperature versus N for the interacting (full curve) and non-interacting (broken line) cases [3].

temperature of approximately 100 nK (see below). The inset to figure 1 compares $\tilde{n}(r)$ and $n_c(r)$ at $T = 75$ nK. The trapped atomic gas has a two-component structure [1, 12] at elevated temperatures, with a relatively dense core of condensed atoms sitting on top of a diffuse cloud of excited atoms with a long tail. Although the non-condensate density in figure 1(b) looks

small in comparison with the condensate, both have an approximately equal number of atoms at this temperature because of the r^2 weighting of the integrated density. We also see that $\tilde{n}(\mathbf{r})$ develops a peak at the edge of the condensate with increasing temperature. This is the analogue of the sharp peak found in the semiclassical Thomas–Fermi approximation [12] in which the condensate has a sharp cut-off at some radius R_0 .

In figure 2(a) we show the total number of atoms N_0 in the condensate as a function of temperature for $N = 2000$ atoms. It can be seen that N_0 is falling to zero at approximately 100 nK, which is close to the BEC transition temperature T_c predicted by the semiclassical approximation [13, 14]. Although there is no sharp transition for a finite system, there is still a characteristic temperature above which N_0 is small. One way of defining this temperature is to fit the temperature variation of N_0 to the functional form $N_0(T) = N_0(0)[1 - (T/T_c)^\alpha]$, treating T_c and α as fitting parameters. As shown in figure 2(a), this functional form provides a reasonable parametrization over a wide intermediate range of temperatures below T_c . The values of T_c extracted in this way are found to scale approximately as $N^{1/3}$, which is the N dependence found for a trapped, non-interacting Bose gas. As can be seen from figure 2(b), the numerical values of T_c found here are slightly smaller than the ideal gas values, in agreement with recent theoretical [15] and experimental [16] results. The value of α extracted from the fits is approximately 2.3 for all values of N studied, as compared with the ideal Bose gas value [14] of 3.

The size of the non-condensate $\tilde{n}(\mathbf{r})$ is, of course, determined by the quasiparticle excitations which deplete the condensate. The mode frequencies for the lowest modes of angular momentum $l = 0, 1$ and 2 are shown in figure 3(a) for a range of temperatures with $N = 2000$ atoms. The $l = 0$ and 2 mode frequencies split apart from the degenerate harmonic potential eigenvalue $2\omega_0$. The $l = 0$ mode is a ‘breathing-type’ mode which is influenced by the compressibility of the condensate, and increases in frequency as a result of the repulsive interactions between the atoms. On the other hand, the $l = 2$ quadrupole mode is a shape resonance and decreases in frequency with increasing N .

The lowest-lying $l = 1$ mode is the centre-of-mass mode of the condensate. It lies very close to, but not exactly at, ω_0 . According to the generalized Kohn theorem for parabolic confinement [17], one would expect an $l = 1$ mode at precisely ω_0 corresponding to a rigid oscillation of the entire trapped gas. This property is satisfied in the Bogoliubov approximation [10, 11] in which all particles are in the condensate. However, in the HFB–Popov approximation, the condensate is effectively moving in the presence of the ‘external’ potential $V_{\text{ext}}(\mathbf{r}) + 2U_0\tilde{n}(\mathbf{r})$, which deviates from the ideal parabolic form. The generalized Kohn theorem is very nearly satisfied because at low temperature $2U_0\tilde{n}(\mathbf{r})$ is only a relatively small perturbation upon the effective potential. Hence the $l = 1$ centre-of-mass mode has a frequency of almost exactly ω_0 . At higher temperatures, although the non-condensate density becomes large, its profile is broad and flat over the region occupied by the condensate. This leads to a uniform shift in the effective potential, which maintains its parabolic character; the generalized Kohn theorem is thus still approximately obeyed.

An improved approximation in which the dynamics of the non-condensate is treated on an equal footing with that of the condensate is needed to recover the true centre-of-mass mode in which both components of the density oscillate together. This also has potential implications for comparison with experimental data as will be discussed later.

2.3. Results for JILA experiment

The validity of the HFB–Popov equations is most stringently tested by comparing shifts in excitation energies as a function of temperature. Such shifts were recently measured at JILA

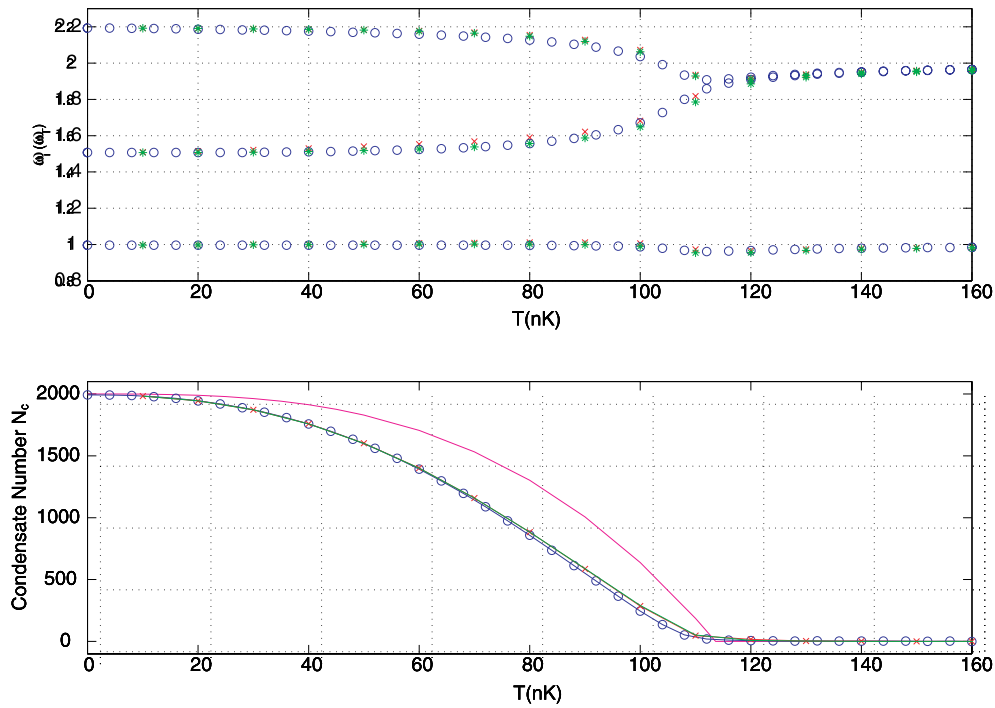


Figure 3. The calculated excitation frequencies for 2000 ^{87}Rb atoms in a 200 Hz spherical harmonic trap. The ideal gas (full curve), GHBF (+), HFB (\times) and HFB–Popov (\circ) results.

[7]. We have solved the HFB–Popov equations under conditions appropriate to this experiment (in particular, in an anisotropic trap) using an iterative procedure. Figure 4 shows the results of the comparison of the experimental temperature-dependent excitation spectrum of a cold-atom cloud contained in the JILA TOP trap, as presented in [7] (full circles) versus the HFB–Popov predictions for the $m = 0$ and 2 modes. The horizontal axis is the absolute temperature scaled by the critical temperature of an ideal Bose gas having the same number of atoms as the trapped cloud given by $T' = T/T_c^0(N)$ where $T_c^0(N) = (\hbar\bar{\omega}/k_B)(N/\zeta(3))^{1/3}$ and $\bar{\omega} = (\omega_\rho^2\omega_z)^{1/3}$ [14]. The vertical axis is the excitation frequency expressed in units of the radial trap frequency.

The HFB–Popov results were obtained using the experimentally determined temperature and a value of μ that produced the experimentally determined total number of atoms, N . Thus there are no adjustable parameters in this calculation. The agreement between theory and experiment is very good (on the order of 5%) for low and intermediate temperatures ($T' \leq 0.6$). As the temperature increases the HFB–Popov excitation frequencies increasingly diverge from the experimental data. This feature of the comparison holds true for both the $m = 0$ and 2 modes.

The behaviour of the HFB–Popov excitation frequencies can be understood in a simple way. The HFB–Popov theory can be used to determine the equation of state for state variables (N, N_0, T) . From this, given the values of N and T , one can determine N_0 . For a fixed total number, this relationship is given by the condensate fraction as a function of T . One can easily predict the temperature-dependent mode frequencies for a particular cold-atom cloud merely by finding the number of condensate atoms, N_0 , in a cloud at the given temperature and

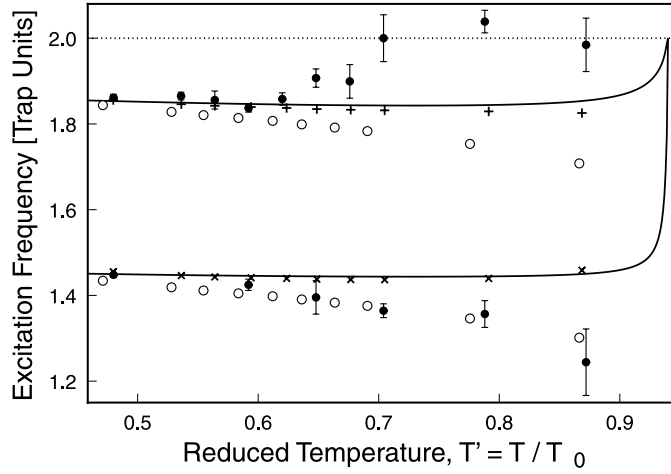


Figure 4. The experimental, temperature-dependent excitation spectrum in the JILA TOP trap (full circles) versus the HFB–Popov predictions for the $m = 0$ mode (top, labelled by ‘+’) and the $m = 2$ mode (bottom, labelled by ‘x’) and the GHFB results (‘o’). The full curves are excitation frequencies for a *zero-temperature* condensate having the same number of condensate atoms as the experimental condensate in the finite- T cloud.

then finding the *zero-temperature* frequency of a condensate of this size. The two full curves in figure 4 are the frequencies determined by the same procedure except that the number of condensate atoms was taken from experiment.

As figure 4 clearly shows, the HFB–Popov solutions reproduce the experimental results quite well when $T \leq 0.6T_c^0(N)$, but fail to reproduce the excitation frequencies at higher temperatures. One possible reason for this failure of the HFB–Popov theory is that it does not account for density variations in the thermal cloud. The thermal density is assumed to be stationary. This is what leads to the violation of the generalized Kohn theorem as discussed in the previous section. In actual experiments the thermal cloud could be driven by the same force as that which drives the condensate. The thermal and condensate modes will also, in general, be coupled. This means that the frequencies calculated from the HFB–Popov approximation will only correspond to the experimentally measured ones if the condensate is driven in such a way as *not* to perturb the thermal density. An alternative problem is due to the omission of terms due to the Popov approximation. In the Popov approximation the anomalous density $\langle \tilde{\psi}(\mathbf{r}) \tilde{\psi}(\mathbf{r}) \rangle$ is assumed to be zero. This is equivalent to assuming that correlations between the particles can be neglected. At higher temperatures, where there is a significant fraction of atoms in the thermal cloud, this is not necessarily the case. It is the inclusion of these two-particle correlations that we now consider.

3. Beyond Popov: HFB?

If we *do not* make the Popov approximation then the condensate wavefunction obeys a generalized Gross–Pitaevskii equation with an additional term containing the *anomalous* average of the field operator $\tilde{m}(\mathbf{r}) \equiv \langle \tilde{\psi}(\mathbf{r}) \tilde{\psi}(\mathbf{r}) \rangle$,

$$\left\{ -\frac{\hbar^2}{2m} \nabla^2 + V_{\text{ext}}(\mathbf{r}) + U_0[n_c(\mathbf{r}) + \tilde{m}(\mathbf{r}) + 2\tilde{n}(\mathbf{r})] \right\} \Phi(\mathbf{r}) = \mu \Phi(\mathbf{r}). \quad (45)$$

The collective excitations are given by the modified BdG equations [5]

$$\begin{aligned}\hat{\mathcal{L}}u_i(\mathbf{r}) - U_0[n_c(\mathbf{r}) + \tilde{m}(\mathbf{r})]v_i(\mathbf{r}) &= E_i u_i(\mathbf{r}) \\ \hat{\mathcal{L}}v_i(\mathbf{r}) - U_0[n_c(\mathbf{r}) + \tilde{m}(\mathbf{r})]u_i(\mathbf{r}) &= -E_i v_i(\mathbf{r})\end{aligned}\quad (46)$$

with

$$\hat{\mathcal{L}} \equiv -\frac{\hbar^2}{2m}\nabla^2 + V_{\text{ext}}(\mathbf{r}) + 2U_0(n_c(\mathbf{r}) + \tilde{n}(\mathbf{r})) - \mu. \quad (47)$$

The anomalous average can be calculated in terms of the quasiparticle transformation functions $u_j(\mathbf{r})$, $v_j(\mathbf{r})$ and populations $N_{\text{Bose}}(E_j)$ using the expression

$$\tilde{m}(\mathbf{r}) = \sum_j u_j(\mathbf{r})v_j^*(\mathbf{r}) [2N_{\text{Bose}}(E_j) + 1]. \quad (48)$$

The above equations form the basis of the HFB theory beyond the Popov approximation.

Unfortunately, there are a number of difficulties with the full HFB theory, notably the appearance of infrared and ultraviolet divergences and the failure of the theory to predict a gapless spectrum. Ultraviolet divergences appear in the expression for the anomalous average of equation (48) as the sum is not convergent at its upper limit if a contact interaction is used to calculate the quasiparticle amplitudes $u_j(\mathbf{r})$ and $v_j^*(\mathbf{r})$. To go beyond the HFB–Popov theory, we need to remove this ultraviolet divergence[†]. To do this we renormalize \tilde{m} by subtracting its value in the two-body perturbative limit. This subtraction can be motivated by noting that the physical interpretation of the anomalous average is that it modifies particle interactions and introduces the many-body T -matrix (see section 4). This T -matrix includes effects of the medium on the scattering of two particles, but also contains two-body effects which exist even in vacuum. These vacuum contributions have already been included in the theory, however, because they are contained in the measured value of the scattering length which appears in the interaction strength U_0 . The renormalization of the anomalous average ensures that these two-body effects are not counted twice [19].

In fact, the simplest way to implement the renormalization numerically is to remove the zero-temperature component of $\tilde{m}(\mathbf{r})$ (i.e. neglect the 1 in the $[2N_{\text{Bose}}(E_i) + 1]$ term of equation (48)), since this contains the divergent part. This procedure is not quite correct as it neglects the contribution from many-body effects at zero temperature. These are extremely small, however, and at temperatures where the corrections from \tilde{m} are important it is calculated to an excellent approximation.

The renormalization of \tilde{m} removes the ultraviolet divergences in the HFB theory, but leaves the problems of infrared divergences and the appearance of a gap in the excitation spectrum. Infrared divergences occur if the energy shifts produced by \tilde{m} are calculated using ordinary perturbation theory. In the homogeneous limit these energy shifts are proportional to \tilde{m}/k in the regime where the wavevector of the excitation satisfies $(\hbar k)^2/2m \ll n_c U_0$. Thus in the infrared limit ($k \rightarrow 0$) the energy shift is divergent. This divergence is removed if equations (45) and (46) are solved self-consistently rather than perturbatively. In this case the resulting excitation spectrum is not gapless, i.e. there is no solution with zero energy. This is problematic because Goldstone’s theorem predicts that there should be such a solution, corresponding to rotations of the condensate phase. In addition, since the HFB–Popov energy spectrum is gapless, the energy shift from the self-consistent calculation, although now finite, is still large compared with the leading-order contribution. The full HFB approach thus leads to incorrect predictions for the low-energy excitation spectrum and cannot be considered to be a well defined theory.

[†] Alternatively one can employ a more complicated pseudopotential as discussed in [18].

The physical reason for these difficulties is the inconsistent treatment of interactions between particles in the HFB approach. We argued above that the anomalous average introduces the many-body T -matrix into the description of particle collisions. However, these corrections only appear in the description of collisions between condensate particles, whereas collisions involving non-condensate particles are described by the two-body T -matrix. On physical grounds, one would expect the effective interaction between any pair of particles to be the same, regardless of whether or not they come from the condensate. This is the case in the HFB–Popov theory where all collisions are described using the two-body T -matrix. An alternative procedure is to include the many-body T -matrix in all collisions. This approach is discussed in the next section, where we motivate the introduction of additional terms into the HFB equations which put many-body effects into collisions involving the non-condensate. The inclusion of these terms produces a gapless HFB theory (GHFB) and removes the difficulties with infrared divergences.

4. The many-body T -matrix and gapless HFB

When two atoms collide their interaction is modified if a condensate is present in two principal ways [20, 21]: (a) the intermediate collisional states may be occupied, leading to a modification of the scattering amplitude via bosonic enhancement and (b) the spectrum of initial, intermediate and final states is altered, i.e. the atoms participating in the collisions are not bare atoms, but dressed ones, or quasiparticles. The medium therefore modifies the effective interaction experienced by a pair of colliding atoms from its value *in vacuo* [22]. These effects lead to the replacement of the two-body T -matrix by the many-body T -matrix [23].

We will now show how the effect of including the many-body T -matrix can be approximated using the anomalous average and how this leads to a new gapless theory [24]. In order to do this we need to write our equations in terms of a basis state expansion. To do this we use an approach based on the linearization of the time-dependent equations of motion. Our time dependent Bose-field operator is then given by

$$\hat{\psi}(\mathbf{r}, t) = \sum_i \phi_i(\mathbf{r}) \hat{a}_i(t). \quad (49)$$

The splitting of the field operator into mean value and fluctuation parts now reads $\hat{a}_i(t) = z_i(t) + \hat{c}_i(t)$. Again we take the average of the fluctuations to vanish, $\langle \hat{a}_i(t) \rangle = z_i(t)$. If we assume only two-body collisions the exact equation of motion for the mean field is

$$i\hbar \frac{d}{dt} z_n(t) = \hbar\omega_n z_n(t) + \sum_{ijk} \langle ni|\hat{V}|jk\rangle \{z_i^*(t)z_j(t)z_k(t) + 2\rho_{ji}(t)z_k(t) + \kappa_{jk}(t)z_i^*(t) + \lambda_{ijk}(t)\}. \quad (50)$$

Here $\hbar\omega_n \delta_{ni} = \langle n|\hat{T}_0|i\rangle = \int \phi_n^*(\mathbf{r}) \hat{T}_0 \phi_i(\mathbf{r}) d\mathbf{r}$ is the matrix for the kinetic energy plus the trap potential, which in the trap basis can be taken to be diagonal. The matrix elements of the interaction terms have been conveniently symmetrized to be $\langle ni|\hat{V}|jk\rangle \equiv \frac{1}{2}[(ni|\hat{V}|jk) + (ni|\hat{V}|kj)]$ with $(ni|\hat{V}|jk) = \iint \phi_n^*(\mathbf{r}) \phi_i^*(\mathbf{r}') \hat{V}(\mathbf{r} - \mathbf{r}') \phi_j(\mathbf{r}) \phi_k(\mathbf{r}') d\mathbf{r} d\mathbf{r}'$. $\rho_{ji}(t)$ is the basis state representation of the pair average $\tilde{n}(\mathbf{r}, t) = \sum_{ij} \phi_i^*(\mathbf{r}) \phi_j(\mathbf{r}) \rho_{ji}(t)$, the anomalous average $\tilde{m}(\mathbf{r}, t)$ is given analogously by $\kappa_{jk}(t)$. We do not assume a contact interaction but keep the full inter-atomic potential \hat{V} . We also do not neglect the triplet anomalous average $\lambda_{ijk}(t) = \langle c_i^\dagger(t) c_j(t) c_k(t) \rangle$. We have argued that the pair correlations are needed to account for collisions between condensate atoms. In order to properly account for the collisions between

condensed and excited atoms one must deal explicitly with correlations of three particles, $\lambda_{ijk}(t)$.

We now linearize the above equation about its static value by writing

$$\psi(\mathbf{r}, t) = [\psi_0(\mathbf{r}) + \delta\psi(\mathbf{r}, t)] e^{-i\mu t}. \quad (51)$$

When allowing the condensate to change in time we must do the same for the correlations between the atoms, so we linearize $\kappa_{ji}(t) = [\kappa_{ji}^0 + \delta\kappa_{ji}(t)] e^{-2i\mu t}$, and $\lambda_{ijk}(t) = [\lambda_{ijk}^0 + \delta\lambda_{ijk}(t)] e^{-i\mu t}$. The HFB approach assumes the populations of the thermal cloud to be static, so we take $\rho_{ij}(t) = \rho_{ij}^0 \delta_{ij} = n_i$. Here n_i are the quasi-particle populations of the respective levels and are given by the Bose–Einstein distribution. We then obtain as the equation for the ground state

$$\mu z_n^0 = \hbar\omega_n z_n^0 + \sum_{ijk} \langle ni | \hat{V} | jk \rangle \{ z_j^0 z_k^0 z_i^{0*} + \kappa_{jk}^0 z_i^{0*} + 2n_i \delta_{ij} z_k^0 + \lambda_{ijk}^0 \} \quad (52)$$

and the following equation for the excitations:

$$\begin{aligned} i\hbar \frac{d}{dt} \delta z_n(t) &= (\hbar\omega_n - \mu) \delta z_n + \sum_{ijk} \langle ni | \hat{V} | jk \rangle \{ z_j^0 z_k^0 \delta z_i^* + \kappa_{jk}^0 \delta z_i^* \} \\ &+ \sum_{ijk} \langle ni | \hat{V} | jk \rangle \{ 2z_i^{0*} z_j^0 \delta z_k + z_i^{0*} \delta \kappa_{jk} \} + \sum_{ijk} \langle ni | \hat{V} | jk \rangle \{ 2n_i \delta_{ij} \delta z_k + \delta \lambda_{ijk} \}. \end{aligned} \quad (53)$$

Using the usual linear response ansatz $\delta z_n(t) = u_{ni} e^{-i\Omega_n t} + v_{ni} e^{i\Omega_n t}$ in the equation for the excitations, we then obtain equations analogous to the coupled HFB equations.

We now make use of the fact that in equation (53) the terms containing anomalous averages modify the interaction potential \hat{V} . The equations of motion for $\kappa_{ij}(t)$ and $\lambda_{ijk}(t)$ can be obtained directly from their commutator with the Hamiltonian. Subsequent linearization then gives the required equations for κ_{ij}^0 , $\delta\kappa_{ij}$, λ_{ijk}^0 and $\delta\lambda_{ijk}$. By way of example we show how the grouping of the average κ_{ij}^0 with the single vertex term of $z_j^0 z_k^0 z_i^{0*}$ in the equation for the static condensate allows us to define an effective interaction. The expression for κ_{ij}^0 reads as follows:

$$\kappa_{jk}^0 = \frac{(1 + n_j + n_k)}{2\mu - \omega_j - \omega_k} \sum_{lm} \langle jk | \hat{V} | lm \rangle [z_l^0 z_m^0 + \kappa_{lm}^0]. \quad (54)$$

This is, in fact, not the full expression for κ_{jk}^0 . We include terms which give ladder interactions to all orders but neglect terms involving higher-order correlations. Inserting this into the equation for the static condensate allows us to write

$$\sum_{ijk} \langle ni | \hat{V} | jk \rangle z_i^{0*} (z_j^0 z_k^0 + \kappa_{jk}^0) = \sum_{ilm} \langle ni | \hat{T}_{\text{MB}} | lm \rangle z_i^{0*} z_m^0 z_l^0 \quad (55)$$

where we have defined to all orders the many-body T -matrix, the effective interaction, according to the recursive Lipmann–Schwinger equation:

$$\hat{T}_{\text{MB}} = \hat{V} + \sum_{jk} \hat{V} | jk \rangle \frac{(1 + n_j + n_k)}{2\mu - \omega_j - \omega_k} \langle jk | \hat{T}_{\text{MB}}. \quad (56)$$

All other correlation terms can be grouped to effective interactions in a similar fashion. The κ terms give rise to effective interactions for condensate–condensate collisions and λ introduces

them for collisions between condensate and excited atoms. The equations for the ground state and the excitations then become

$$0 = (\hbar\omega_n - \mu) z_n^0 + \sum_{ijk} \langle ni | \hat{T}_{\text{MB}} | jk \rangle z_j^0 z_k^0 z_i^{0*} + \sum_{ik} 2n_i \langle ni | \hat{T}_{\text{MB}} | ik \rangle z_k^0 \quad (57)$$

$$\begin{aligned} i\hbar \frac{d}{dt} \delta z_n(t) &= (\hbar\omega_n - \mu) \delta z_n(t) + \sum_{ijk} \langle ni | \hat{T}_{\text{MB}} | jk \rangle z_j^0 z_k^0 \delta z_i^*(t) \\ &+ \sum_{ijk} 2 \langle ni | \hat{T}_{\text{MB}} | jk \rangle z_i^{0*} z_j^0 \delta z_k(t) + \sum_{ik} 2n_i \langle ni | \hat{T}_{\text{MB}} | ik \rangle \delta z_k(t). \end{aligned} \quad (58)$$

We have thus obtained a set of equations that supports a zero-frequency mode with $[u_0(\mathbf{r}), v_0(\mathbf{r})] = [\psi_0(\mathbf{r}), -\psi_0^*(\mathbf{r})]$ and the theory is thus termed gapless.

It is convenient to express $\langle \hat{T}_{\text{MB}} \rangle$ in terms of contact interactions. We shall use \tilde{U}_{con} to describe collisions between condensate atoms and \tilde{U}_{exc} for the terms describing collisions between condensed and excited particles. In general, the two effective interactions are momentum dependent and they need not necessarily be the same. We should expect the interaction between condensed and excited atoms to be similar to that between two condensate atoms, as long as the change in relative momenta of the colliding particles between the two cases is not too great. This is the version of the theory we use in this paper, upgrading U_0 to $\langle \hat{T}_{\text{MB}} \rangle$ everywhere in the HFB–Popov equations. In the limit of high relative momenta the condensate–excited-state interactions are best described by the two-body T -matrix since many-body effects die out in this regime. We do not treat this scenario explicitly in this work.

If we assume $\langle \hat{T}_{\text{MB}} \rangle$ to be roughly momentum independent we can use $\langle 00 | \hat{T}_{2\text{B}} | 00 \rangle = U_0 \delta(\mathbf{r} - \mathbf{r}')$, where $U_0 = 4\pi\hbar^2 a/m$ is the usual dilute Bose gas effective interaction strength, to write

$$\begin{aligned} \langle \hat{T}_{\text{MB}} \rangle &\simeq \langle 00 | \hat{T}_{\text{MB}} | 00 \rangle = \langle 00 | \hat{T}_{2\text{B}} + \sum_{ij} \hat{T}_{2\text{B}} | ij \rangle \frac{[1 + n_j + n_i]}{(2\mu - \omega_i - \omega_j)} \langle ij | \hat{T}_{\text{MB}} | 00 \rangle \\ &\rightarrow U_0 \left[1 + \frac{\tilde{m}(\mathbf{r})}{\psi^2(\mathbf{r})} \right]. \end{aligned} \quad (59)$$

We therefore substitute $\tilde{U}_0(\mathbf{r}) = \tilde{U}_{\text{con}} = \tilde{U}_{\text{exc}} = U_0 [1 + \tilde{m}/\psi^2]$ everywhere in the HFB–Popov theory [25].

5. Results using GHFB

Having developed a gapless theory [25] that takes into account the effects of two-particle correlations, we now examine quantitatively what effects those correlations have. Let us first return to the case of the 200 Hz spherical trap. Again we initially consider the case of 2000 rubidium atoms. At $T = 0$ the anomalous average is approximately zero and we hence obtain identical results to HFB–Popov. As the temperature is increased, so the magnitude of the anomalous average increases as the non-condensed states become populated. For the 2000-atom case the non-condensate density profiles and anomalous density profiles are shown in figures 5(a) and (b), respectively, at temperature of 20, 40, 60, 80 and 100 nK. Although the non-condensate density, of course, increases monotonically with temperature, at temperatures approaching T_c , the anomalous average begins to decrease. This is because of the large depletion of the condensate. At temperatures greater than the transition temperature

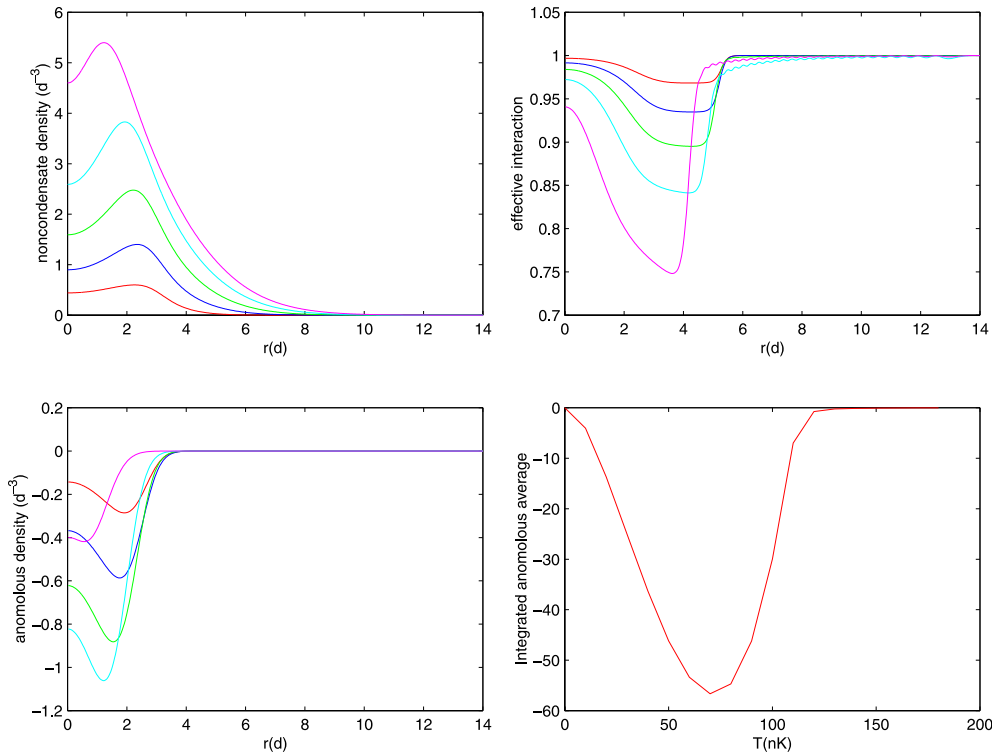


Figure 5. (a) Non-condensate density as a function of position for the spherical trap with 2000 rubidium atoms at temperatures of 20, 40, 60, 80 and 100 nK. (b) Anomalous density profiles for the same temperatures. (c) The integrated anomalous density as a function of temperature. (d) The spatially dependent effective interaction for the same range of temperatures.

the anomalous average goes to zero. The integrated value of the anomalous average is shown in figure 5(d). The maximal (absolute) value of the anomalous average occurs when there are approximately equal non-condensate and condensate populations. So how is the effective interaction between the particles modified? As \tilde{m} becomes more negative with temperature the spatially dependent effective interaction, $\tilde{U}_0(r)$, develops a dip near the edge of the condensate. Far away from the condensate \tilde{U}_0 returns to the vacuum value of U_0 . At its greatest depletion in the case studied here the minimum in \tilde{U}_0 was reduced to approximately 75% of its vacuum value. The effect of this reduction upon the condensate fraction and excitation frequencies is surprisingly small in the isotropic case, however. Figure 4 shows the excitation frequencies and condensate fraction for both the HFB–Popov calculation and for the GHFB calculation. There is clearly very little difference. Even for calculations involving much larger numbers of atoms (up to 10 000 or 20 000 atoms) the differences never exceeded 1%.

In the case of the anisotropic trap corresponding to the JILA experiment, we again see that there are virtually no effects due to pair correlations for temperatures below about $0.6T_c$. This is the region in which the HFB–Popov calculations agree well with the experimental data. However, the inclusion of correlations does have an effect precisely in the region where the experimental results begin to deviate from the HFB–Popov theory. Replacing the two body T -matrix with the many body T -matrix produces a downward shift in the excitation spectrum

for both the $m = 0$ and 2 excitations. The size of the shift increases as one approaches T_c up to a maximum of order 10%. The shift is in *quantitative* agreement with the experimental data for the $m = 2$ mode (figure 3). It therefore appears that the inclusion of correlations between particles in the inter-particle scattering accounts well for the shifts in the lower-lying excitation of the JILA experiment. This does not explain the shift in the $m = 0$ mode, however. Although the onset of the shift away from the excitation frequencies of the HFB–Popov calculation is in the same region for both the experimental data and the GHFB calculation, the shifts are of opposite sign. It is assumed therefore that the shift in the $m = 0$ mode observed in the experiment may be due to some dynamical behaviour of the non-condensate not included in the present calculation. Encouraged by the excellent agreement with the lower mode, however, perhaps further experimental investigation of the excitation spectra of these systems would be fruitful in helping to understand what validity the finite-temperature mean-field theory calculations have for the upper mode.

6. Conclusions

In this paper we have shown in detail how to formally develop a self-consistent finite-temperature field theory treatment of the Bose–Einstein condensation of trapped dilute atomic gases. We have shown that the simplest such theory that satisfies Goldstone’s theorem is the Popov approximation to the Hartree–Fock–Bogoliubov formalism. The numerical methods for implementing this formalism, in both an isotropic trap and an anisotropic trap corresponding to real experiments, have been expounded and a detailed comparison with experiment has been made. The results are excellent for temperatures below about $0.6T_c$. As the critical temperature is approached, however, the calculated excitation frequencies diverge from those measured in the JILA experiment.

We have therefore discussed possible problems with the theory, highlighting the facts that the dynamics of the non-condensate are neglected and that two-body correlations are not described in a complete manner. To address the first of these points would require a new significant extension to the formalism. This is described by Morgan elsewhere in this issue [26]. We have therefore focused upon the second point. The anomalous average, neglected in the Popov approximation, was identified as the quantity that represents two-body correlations. To go beyond the HFB–Popov treatment, one must include this term. This presents some difficulty as the usual HFB formulation has a gap in the excitation spectrum, violating Goldstone’s theorem. The source of this failure was identified and the correct method of including correlations (the replacement of the two-body T -matrix by the many-body T -matrix everywhere) expounded in detail, together with a derivation of an expression for the many-body T -matrix in terms of the anomalous average. Other problems concerning infrared and ultraviolet divergences were addressed.

The results of the new gapless HFB theory were again compared with experiment. The small corrections at higher temperatures brought the theory into agreement with the measured values for the $m = 2$ mode at least. Problems remain in the understanding of the behaviour of the higher-lying $m = 0$ mode, however. The resolution of this problem may lie with our knowledge of exactly what is happening in the experiments or with the fact that the theory does not include the dynamics of the thermal cloud. Further experiments are needed to clarify this, as is further theoretical work to include the higher-order terms required to represent these dynamics [27, 28].

Acknowledgments

This work was supported by grants from the Engineering and Physical Sciences Research Council of the United Kingdom, US National Science Foundation Grant nos PHY-9601261 and PHY-9612728, the Natural Sciences and Engineering Research Council of Canada, and the Alexander S Onassis Public Benefit Foundation (Greece). We would like to thank Allan Griffin for many useful discussions and his help in preparing this manuscript.

Appendix. Numerical solution of the HFB–Popov equations

The HFB–Popov equations, in this work, have been solved numerically differently according to whether the harmonic trap potential confining the gas was isotropic or anisotropic. In both methods the solutions are expanded in basis-set functions and the resulting matrix eigenvalue problems are solved by standard techniques. Using a basis set consisting of eigenstates of the combined potential due to the trap and the mean field of the condensate in the isotropic case yields an efficient numerical solution. Calculation of corresponding eigenstates in the anisotropic case becomes very expensive and so a basis set consisting of eigenstates of the trap potential alone must be used. We describe both methods in detail below.

A.1. Isotropic trap

The basic equations that must be solved are the uncoupled equations (equations (40) and (41))

$$(\hat{h}_0 - \mu)^2 \psi_i^{(+)}(\mathbf{r}) + 2U_0 n_c(\mathbf{r})(\hat{h}_0 - \mu) \psi_i^{(+)}(\mathbf{r}) = E_i^2 \psi_i^{(+)}(\mathbf{r}) \quad (\text{A1})$$

$$(\hat{h}_0 - \mu)^2 \psi_i^{(-)}(\mathbf{r}) + 2U_0(\hat{h}_0 - \mu)n_c(\mathbf{r})\psi_i^{(-)}(\mathbf{r}) = E_i^2 \psi_i^{(-)}(\mathbf{r}) \quad (\text{A2})$$

and the solutions are related to each other by $(\hat{h}_0 - \mu)\psi_i^{(+)} = E_i \psi_i^{(-)}$.

To solve equations (A1) and (A2), we define the normalized eigenfunctions of the Hamiltonian \hat{h}_0 by

$$(\hat{h}_0 - \mu)\phi_\alpha(\mathbf{r}) = \varepsilon_\alpha \phi_\alpha(\mathbf{r}). \quad (\text{A3})$$

The lowest energy solution of equation (A3) defines the condensate wavefunction $\phi_0(\mathbf{r})$ with eigenvalue $\varepsilon_0 = \epsilon_0(N_0) - \mu$. More generally, the eigenvalues ε_α are shifted by μ with respect to the eigenvalues ϵ_α of \hat{h}_0 . We use this basis to expand $\psi_i^{(+)}(\mathbf{r})$ as

$$\psi_i^{(+)}(\mathbf{r}) = \sum_{\alpha} c_{\alpha}^{(i)} \phi_{\alpha}(\mathbf{r}) \quad (\text{A4})$$

where, in keeping with equation (5), the state $\phi_0(\mathbf{r})$ is excluded from the expansion. Substituting this result into equation (A1), we obtain the eigenvalue equation

$$\sum_{\beta} \{M_{\alpha\beta} + \varepsilon_{\alpha} \delta_{\alpha\beta}\} \varepsilon_{\beta} c_{\beta}^{(i)} = E_i^2 c_{\alpha}^{(i)} \quad (\text{A5})$$

where the matrix $M_{\alpha\beta}$ is defined as

$$M_{\alpha\beta} = 2U_0 \int d\mathbf{r} \phi_{\alpha}^*(\mathbf{r}) n_c(\mathbf{r}) \phi_{\beta}(\mathbf{r}). \quad (\text{A6})$$

Equation (A5) can be put into a symmetrical form by means of the transformation $\mathbf{w}^{(i)} = \mathcal{D}^{1/2} \mathbf{c}^{(i)}$, where \mathcal{D} is the diagonal matrix $D_{\alpha\beta} = \varepsilon_{\alpha} \delta_{\alpha\beta}$. We then have

$$(\mathcal{D}^2 + \mathcal{D}^{1/2} \mathcal{M} \mathcal{D}^{1/2}) \mathbf{w}^{(i)} = E_i^2 \mathbf{w}^{(i)}. \quad (\text{A7})$$

The matrix multiplying the vector $w^{(i)}$ is Hermitian and the eigenvalues E_i^2 are real. Furthermore, since the matrix $(\mathcal{M} + \mathcal{D})$ is positive definite, the eigenvalues E_i^2 are positive and hence the E_i are real. In a similar way, the function $\psi_i^{(-)}(\mathbf{r})$ can be expanded as

$$\psi_m^{(-)}(\mathbf{r}) = \sum_{\alpha} d_{\alpha}^{(i)} \phi_{\alpha}(\mathbf{r}) \quad (\text{A8})$$

where the expansion coefficients are given by

$$d_{\alpha}^{(i)} = \frac{\varepsilon_{\alpha}}{E_i} c_{\alpha}^{(i)}. \quad (\text{A9})$$

Finally, we note that the original Bogoliubov amplitudes are given by

$$\begin{aligned} u_i(\mathbf{r}) &= \frac{1}{2} \sum_{\alpha} \left(1 + \frac{\varepsilon_{\alpha}}{E_i}\right) c_{\alpha}^{(i)} \phi_{\alpha}(\mathbf{r}) \\ v_i(\mathbf{r}) &= \frac{1}{2} \sum_{\alpha} \left(1 - \frac{\varepsilon_{\alpha}}{E_i}\right) c_{\alpha}^{(i)} \phi_{\alpha}(\mathbf{r}). \end{aligned} \quad (\text{A10})$$

These functions satisfy the orthonormality conditions

$$\int d\mathbf{r} [u_i^*(\mathbf{r})u_j(\mathbf{r}) - v_i^*(\mathbf{r})v_j(\mathbf{r})] = \delta_{ij} \quad (\text{A11})$$

which implies that the $c_{\alpha}^{(i)}$'s are normalized according to

$$\sum_{\alpha} \varepsilon_{\alpha} c_{\alpha}^{(i)*} c_{\alpha}^{(j)} = E_i \delta_{ij}. \quad (\text{A12})$$

This equation is consistent with the fact that equation (A7) defines a Hermitian eigenvalue problem, and hence the eigenvectors $w^{(i)}$ are orthogonal, $\sum_{\alpha} w_{\alpha}^{(i)*} w_{\alpha}^{(j)} \propto \delta_{ij}$.

The non-condensate density defined in equation (33) consists of a part

$$\tilde{n}_1(\mathbf{r}) = \sum_i [|u_i(\mathbf{r})|^2 + |v_i(\mathbf{r})|^2] N_{\text{Bose}}(E_i) \quad (\text{A13})$$

which vanishes in the $T \rightarrow 0$ limit and a part

$$\tilde{n}_2(\mathbf{r}) = \sum_i |v_i(\mathbf{r})|^2 \quad (\text{A14})$$

which is finite in this limit. The latter then represents the non-condensate density in the ground state of the system. However, $\tilde{n}_2(\mathbf{r})$ is a function of temperature as a result of the temperature dependence of $\hat{\mathcal{L}}$ and $n_c(\mathbf{r})$ which determines the function v_i .

In terms of the coefficients $c_{\alpha}^{(i)}$, we have the explicit expressions

$$\tilde{n}_1(\mathbf{r}) = \frac{1}{2} \sum_i \left\{ \left| \sum_{\alpha} c_{\alpha}^{(i)} \phi_{\alpha}(\mathbf{r}) \right|^2 + \left| \sum_{\alpha} \frac{\varepsilon_{\alpha}}{E_i} c_{\alpha}^{(i)} \phi_{\alpha}(\mathbf{r}) \right|^2 \right\} N_{\text{Bose}}(E_i) \quad (\text{A15})$$

and

$$\tilde{n}_2(\mathbf{r}) = \frac{1}{4} \sum_i \left| \sum_{\alpha} \left(1 - \frac{\varepsilon_{\alpha}}{E_i}\right) c_{\alpha}^{(i)} \phi_{\alpha}(\mathbf{r}) \right|^2. \quad (\text{A16})$$

The total number of particles out of the condensate is obtained by integrating these expressions over all space. We then have

$$\begin{aligned} \tilde{N}_1 &= \frac{1}{2} \sum_i \sum_{\alpha} \left(1 + \frac{\varepsilon_{\alpha}^2}{E_i^2}\right) |c_{\alpha}^{(i)}|^2 N_{\text{Bose}}(E_i) \\ \tilde{N}_2 &= \frac{1}{4} \sum_i \sum_{\alpha} \left(1 - \frac{\varepsilon_{\alpha}}{E_i}\right)^2 |c_{\alpha}^{(i)}|^2. \end{aligned} \quad (\text{A17})$$

A.2. Anisotropic trap

We have also solved HFB–Popov equations under conditions appropriate to the JILA experiment [7] using an iterative procedure. Each iteration consisted of two parts: (a) solving the generalized GP equation (equation (22)) using the value of $\tilde{n}(\mathbf{r})$ from the previous iteration, which yields $\Phi(\mathbf{r})$ and a new value of N_0 from normalization; (b) solving the coupled HFB–Popov equations (equations (29)) using $\Phi(\mathbf{r})$ from step (a) and $\tilde{n}(\mathbf{r})$ from the previous iteration. This yields the $\{u_j(\mathbf{r})\}$, $\{v_j(\mathbf{r})\}$ and $\{E_j\}$ which are then used in equation (33) to update $\tilde{n}(\mathbf{r})$. The total number of trapped atoms, N , is updated by integrating \tilde{n} over all space and adding this to N_0 . Convergence is reached when the change in N from one iteration to the next is smaller than a specified tolerance.

To perform step (a), we use the basis-set method. The solution of equation (22) is expanded in a finite basis of eigenfunctions of the trap potential, $\Phi(\mathbf{r}) = \sum_k c_k \phi_k(\mathbf{r})$, and the scalar product of the result is taken with each ϕ_k . Since \tilde{n} comes from the previous self-consistent iteration, equation (22) is similar to the zero-temperature GP equation and can be solved by Newton–Raphson iteration.

Step (b) is performed by expanding the quasi-particle amplitudes in trap eigenfunctions, $u_j(\mathbf{r}) = \sum_i a_i^{(j)} \phi_i(\mathbf{r})$ and $v_j(\mathbf{r}) = \sum_i b_i^{(j)} \phi_i(\mathbf{r})$. Insertion of these expansions in equations (29) yields a generalized matrix eigenvalue problem for the coefficients $\{a_i^{(j)}\}$ and $\{b_i^{(j)}\}$. The size of the matrix problem can be significantly reduced using rotational and reflection symmetry about the trap axis. Thus each quasi-particle amplitude pair $\{u_j(\mathbf{r}), v_j(\mathbf{r})\}$ will have a definite value of the azimuthal quantum number m and will be even or odd under the reflection $z \rightarrow -z$. Hence the quasi-particle index j can be replaced with the set $\{m, \pm, q\}$ (below we label states within a subspace of fixed m , z -parity, and q). The generalized matrix eigenvalue problem can be recast as an ordinary eigenvalue problem for the *squares* of E_j within each subspace of fixed m and z -parity using the following decoupling transformation: $(\mathbf{s}_q)_p \equiv a_p^{(q)} + b_p^{(q)}$ and $(\mathbf{d}_q)_p \equiv a_p^{(q)} - b_p^{(q)}$, where \mathbf{s}_q and \mathbf{d}_q denote column vectors. This decoupling transformation is equivalent to that used in [3] except that it appears here within the context of basis-set expansion coefficients. The form of the eigenvalue equations actually solved are

$$A_- A_+ \mathbf{s}_q = E_q^2 \mathbf{s}_q \quad \mathbf{d}_q = \frac{1}{E_q} A_+ \mathbf{s}_q \quad (\text{A18})$$

the matrices A_\pm are given by $(A_\pm)_{pp'} = (\epsilon_p - \mu) \delta_{pp'} + U_0 [N_0 (2 \pm 1) \rho_{pp'} + 2\tilde{n}_{pp'}]$, where $\rho_{pp'}$ and $\tilde{n}_{pp'}$ are matrix elements of $\phi(\mathbf{r})$ and $\tilde{n}(\mathbf{r})$ within the basis set, respectively.

We have checked our numerical results in several ways. First, we have reproduced the results of [3]. We have verified that the ideal gas result is recovered when the scattering length is set to zero. Finally, we have written two completely independent versions of the code and have checked that they produce the same answers.

We should note that the convergence problems in the excitation frequencies at high temperatures, discussed in [3], were avoided simply by adding a correction to the total number of atoms, N , at each iteration. For high-energy oscillator eigenfunctions, the overlaps of the quasi-particle amplitudes with the condensate wavefunction are negligible. These amplitudes do not modify the low-lying excitation frequencies but do contribute to N . Furthermore, the $\{u_j\}$ and $\{v_j\}$ approach oscillator eigenstates and zero, respectively, as ϵ_j becomes large, while the eigenvalues behave as $E_j \rightarrow \epsilon_j - \mu$, where ϵ_j is the oscillator energy eigenvalue. Hence a sum over Bose–Einstein factors of the form $\sum_{j, \epsilon_j > \epsilon_{\max}} (e^{\beta E_j} - 1)^{-1}$ is added to the N calculated by integration of \tilde{n} computed within the truncated basis set. The energy cut-off, ϵ_{\max} , is chosen to converge the condensate fraction and low-lying excitation frequencies.

References

- [1] Anderson M H *et al* 1995 *Science* **269** 198
- [2] Mewes M O *et al* 1996 *Phys. Rev. Lett.* **77** 992
- [3] Hutchinson D A W, Zaremba E and Griffin A 1997 *Phys. Rev. Lett.* **78** 1842
- [4] Dodd R J, Edwards M, Clark C W and Burnett K 1998 *Phys. Rev. A* **57** R32
- [5] Griffin A 1996 *Phys. Rev. B* **53** 9341
- [6] Griffin A 1999 *Bose–Einstein Condensation in Atomic Gases (Proc. Int. School of Physics ‘Enrico Fermi’ Course CXL)* ed M Inguscio, S Shingari and C E Wieman (Amsterdam: IOS)
- [7] Jin D S, Matthews M R, Ensher J R, Wieman C E and Cornell E A 1997 *Phys. Rev. Lett.* **78** 764
- [8] Goldstone J 1961 *Nuovo Cimento* **19** 154
- [9] Edwards M *et al* 1996 *Phys. Rev. Lett.* **77** 1671
- [10] Singh K G and Rokhsar D S 1996 *Phys. Rev. Lett.* **77** 1667
- [11] Stringari S 1996 *Phys. Rev. Lett.* **77** 2360
- [12] Goldman V V, Silvera I F and Leggett A J 1981 *Phys. Rev. B* **24** 2870
- [13] de Groot S R, Hooyman G J and Ten Seldam C A 1950 *Proc. R. Soc. A* **203** 266
- [14] Bagnato V, Pritchard D E and Kleppner D 1987 *Phys. Rev. A* **35** 4354
- [15] Giorgini S, Pitaevskii L P and Stringari S 1996 *Phys. Rev. A* **54** 4633R and private communication
- [16] Mewes M O *et al* 1996 *Phys. Rev. Lett.* **77** 416
Ensher J R *et al* 1996 *Phys. Rev. Lett.* **77** 4984
- [17] See Dobson J F 1994 *Phys. Rev. Lett.* **73** 2244 and references therein
- [18] Huang K and Tommasini P 1996 *J. Res. Natl Inst. Stand. Technol.* **101** 435 and references therein
- [19] Lifshitz E M and Pitaevskii L P 1980 *Statistical Physics Part 2, Landau and Lifshitz Course of Theoretical Physics* vol 9 (Oxford: Pergamon)
- [20] Shi H and Griffin A 1998 *Phys. Rep.* **304** 1
- [21] Proukakis N P, Burnett K and Stoof H T C 1998 *Phys. Rev. A* **57** 1230
- [22] Proukakis N P and Burnett K 1997 *Phil. Trans. R. Soc. A* **355** 2235
- [23] Stoof H T C, Bijlsma M and Houbiers M 1996 *J. Res. Natl Inst. Stand. Technol.* **101** 443
- [24] Rusch M and Burnett K 1999 *Phys. Rev. A* **59** 3851
- [25] Hutchinson D A W, Dodd R J and Burnett K 1998 *Phys. Rev. Lett.* **81** 2198
Proukakis N P, Morgan S A, Choi S and Burnett K 1998 *Phys. Rev. A* **58** 2435
- [26] Morgan S A 2000 *J. Phys. B: At. Mol. Opt. Phys.* **33** 3847
(Morgan S A 1999 *Preprint cond-mat/9911278*)
- [27] Rusch M, Morgan S A, Hutchinson D A W and Burnett K to be published
- [28] Zaremba E, Nikuni T and Griffin A 1999 *J. Low Temp. Phys.* **116** 277